Inorg. Chem. **2009**, *48*, 1370−1379

Nonlinear Optical and Related Properties of Iron(II) Pentacyanide Complexes with Quaternary Nitrogen Electron Acceptor Units

Benjamin J. Coe,*,† Simon P. Foxon,† Elizabeth C. Harper,† James Raftery,† Rachel Shaw,† Catherine A. Swanson,† Inge Asselberghs,‡ Koen Clays,‡ Bruce S. Brunschwig,§ and Anthony G. Fitch§

School of Chemistry, University of Manchester, Oxford Road, Manchester M13 9PL, U.K., Department of Chemistry, University of Leuven, Celestijnenlaan 200D, B-3001 Leuven, Belgium, and Molecular Materials Research Center, Beckman Institute, MC 139-74, California Institute of Technology, 1200 East California Boulevard, Pasadena, California 91125

Received July 2, 2008

Three new complex salts $Na_2[Fe^{II}(CN)_5(L)]$ [L = *N*-methyl-4-{*E*,*E*-4-(4-pyridyl)buta-1,3-dienyl}pyridinium, *N*-methyl-4-{*E*,*E*,*E*-6-(4-pyridyl)hexa-1,3,5-trienyl}pyridinium, or *N*-methyl-1,4-bis-{*E*-2-(4-pyridyl)ethenyl}] benzene have been prepared. These compounds have been characterized by using various techniques including electronic absorption spectroscopy and cyclic voltammetry, allowing their properties to be compared with those of the known complexes where L = *N*-methylpyrazinium ($Mepyz^+$), *N*-methyl-4,4′-bipyridinium, or *N*-methyl-4-[*E*-2-(4-pyridyl)ethenyl]pyridinium. Molecular quadratic nonlinear optical (NLO) responses have been determined by using hyper-Rayleigh scattering (HRS) at 1064 nm, and also via Stark (electroabsorption) spectroscopic studies on the intense, visible $d \rightarrow \pi^*$ metal-to-ligand charge-transfer (MLCT) bands. The MLCT transitions show large red-shifts on moving from aqueous to methanol solutions, and these excitations are associated with relatively large static first hyperpolarizabilities β_0. Single crystal X-ray structures of two hydrated materials containing the complex anion $[Fe^{II}(CN)_5(Mepyz^+)]^{2-}$ have been determined, and both of these show some degree of alignment of the constituent complex dipoles.

Introduction

Organic nonlinear optical (NLO) materials have received much attention because of their range of potential applications that includes optical data processing and biological imaging.[1] The first commercialization of such compounds has recently involved crystals of the organic salt *E*-4′-(dimethylamino)-*N*-methyl-4-stilbazolium tosylate (DAST) that can be used for terahertz (THz) wave generation via nonlinear frequency mixing (a quadratic NLO effect).[2] Attractive aspects of such molecular salt compounds include the possibility of exploiting counterion variations to produce non-centrosymmetric bulk crystalline structures which are a prerequisite for macroscopic quadratic (second-order) NLO effects. As a now quite widely studied subclass of NLO compounds, organotransition metal complexes offer extensive opportunities for the creation of new multifunctional materials in which potentially useful optical behavior is combined with redox, magnetic, and other properties.[3] For example, a number of recent studies have involved the use of reversible metal-based redox chemistry to switch different types of NLO phenomena.[4]

Quadratic NLO effects derive at the molecular level from the first hyperpolarizability β which translates into the bulk susceptibility $\chi^{(2)}$ in a polar solid. The simplest and most common type of molecular structure that gives large β values is a highly polarizable dipole which contains strong electron

* To whom correspondence should be addressed. E-mail: b.coe@manchester.ac.uk.
† University of Manchester.
‡ University of Leuven.
§ California Institute of Technology.

(1) (a) *Molecular Nonlinear Optics: Materials, Physics and Devices*; Zyss, J., Ed.; Academic Press: Boston, 1994. (b) *Organic Nonlinear Optical Materials*; Bosshard, Ch., Sutter, K., Prêtre, Ph., Hulliger, J., Flörsheimer, M., Kaatz, P., Günter, P., Eds.; Gordon & Breach: Amsterdam, The Netherlands, 1995; Advances in Nonlinear Optics, Vol. 1. (c) *Nonlinear Optics of Organic Molecules and Polymers*; Nalwa, H. S., Miyata, S., Eds.; CRC Press: Boca Raton, FL, 1997. (d) Marder, S. R. *Chem. Commun.* **2006**, 131. (e) *Nonlinear Optical Properties of Matter: From Molecules to Condensed Phases*; Papadopoulos, M. G., Leszczynski, J., Sadlej, A. J., Eds.; Springer: Dordrecht, 2006.

(2) See, for example: (a) Taniuchi, T.; Ikeda, S.; Okada, S.; Nakanishi, H. *Jpn. J. Appl. Phys.* **2005**, *44*, L652. (b) Schneider, A.; Neis, M.; Stillhart, M.; Ruiz, B.; Khan, R. U. A.; Günter, P. *J. Opt. Soc. Am. B* **2006**, *23*, 1822.

10.1021/ic801224u CCC: $40.75
Published on Web 01/12/2009

donor and acceptor groups connected via an extended π-bridge. Such D-π-A chromophores also exhibit intense intramolecular charge-transfer transitions that generally occur in the visible region. Experimentally measured β values are therefore enhanced to variable degrees by resonance, and the establishment of meaningful molecular structure−activity correlations requires the derivation of static (off-resonance) first hyperpolarizabilities β_0. Because practical applications must avoid any actual absorption of light, β_0 values are the most relevant parameter used to characterize new chromophores. Most metal-based NLO chromophores contain electron-rich metal center(s), so their β responses are associated with metal-to-ligand charge-transfer (MLCT) transitions.

We have studied previously a range of D-π-A chromophores with ruthenium(II) penta/tetraammine centers connected to pyridinium-substituted ligands that show very large β_0 responses.[3m,p,4a,n] In a recent investigation, we extended this work to include the first NLO studies with related complexes containing $\{Fe^{II}(CN)_5\}^{3-}$ as the electron-rich center.[5] The optical properties of these latter chromophores are unusually sensitive to the solvent medium and can also be switched by partial protonation of the cyanide ligands.[5] Although quite a number of earlier reports have described $\{Fe^{II}(CN)_5\}^{3-}$ complexes of pyridyl and related ligands,[6] their scope has often been restricted to solution MLCT spectroscopic and kinetic properties, and structural studies on such species are rare. In the present study, we describe several new complex salts $Na_2[Fe^{II}(CN)_5L]$ (where L is a pyridinium-substituted pyridyl ligand), as well as further investigations involving the well-known complex anion $[Fe^{II}(CN)_5(Mepyz^+)]^{2-}$ ($Mepyz^+$ = *N*-methylpyrazinium). The latter species is shown to form two polar crystalline materials, while the new chromophores contain extended ligand π-conjugated frameworks that give rise to increased molecular NLO responses.

Experimental Section

Materials and Procedures. The pro-ligand salts *N*-methylpyrazinium iodide ($[Mepyz^+]I$),[6d] *N*-methyl-4-{*E*,*E*-4-(4-pyridyl)buta-1,3-dienyl}pyridinium iodide ($[Mebpb^+]I\cdot H_2O$),[7] *N*-methyl-4-{*E*,*E*,*E*-6-(4-pyridyl)hexa-1,3,5-trienyl}pyridinium chloride ($[Mebph^+]Cl\cdot 2.1H_2O$),[7] and *N*-methyl-1,4-bis-{*E*-2-(4-pyridyl)-ethenyl}benzene chloride ($[Mebpvb^+]Cl\cdot H_2O$)[7] were synthesized according to published methods. The complex salt $Na_3[Fe^{II}(CN)_5(NH_3)]$ was obtained from Aldrich and purified by recrystallization from aqueous ammonia/ethanol before use.[5] All other reagents were obtained commercially and used as supplied. Products were dried at room temperature in a vacuum desiccator ($CaSO_4$).

General Physical Measurements. ^1H NMR spectra were recorded on a Bruker UltraShield 500 spectrometer, and all shifts are referenced to TMS. The fine splitting of pyridyl or phenyl ring AA′BB′ patterns is ignored, and the signals are reported as simple doublets, with *J* values referring to the two most intense peaks. Elemental and thermogravimetric analyses (TGA) were performed by the Microanalytical Laboratory, University of Manchester. IR spectra were obtained as KBr discs with an ATI Mattson Genesis Series FTIR instrument, and UV−vis spectra were obtained by

(3) (a) Kanis, D. R.; Ratner, M. A.; Marks, T. J. *Chem. Rev.* **1994**, *94*, 195. (b) Long, N. J. *Angew. Chem., Int. Ed. Engl.* **1995**, *34*, 21. (c) Whittall, I. R.; McDonagh, A. M.; Humphrey, M. G.; Samoc, M. *Adv. Organomet. Chem.* **1998**, *42*, 291. (d) Whittall, I. R.; McDonagh, A. M.; Humphrey, M. G.; Samoc, M. *Adv. Organomet. Chem.* **1998**, *43*, 349. (e) Heck, J.; Dabek, S.; Meyer-Friedrichsen, T.; Wong, H. *Coord. Chem. Rev.* **1999**, *190*−*192*, 1217. (f) Gray, G. M.; Lawson, C. M. In *Optoelectronic Properties of Inorganic Compounds*; Roundhill, D. M., Fackler, J. P., Jr., Eds.; Plenum: New York, 1999; pp 1−27. (g) Shi, S. In *Optoelectronic Properties of Inorganic Compounds*; Roundhill, D. M.; Fackler, J. P., Jr., Eds.; Plenum: New York, 1999; pp 55−105. (h) Le Bozec, H.; Renouard, T. *Eur. J. Inorg. Chem.* **2000**, 229. (i) Barlow, S.; Marder, S. R. *Chem. Commun.* **2000**, 1555. (j) Lacroix, P. G. *Eur. J. Inorg. Chem.* **2001**, 339. (k) Di Bella, S. *Chem. Soc. Rev.* **2001**, *30*, 355. (l) Goovaerts, E.; Wenseleers, W. E.; Garcia, M. H.; Cross, G. H. In *Handbook of Advanced Electronic and Photonic Materials and Devices*; Nalwa, H. S., Ed.; Academic Press: San Diego, 2001; Vol. *9*, pp 127−191. (m) Coe, B. J. In *Comprehensive Coordination Chemistry II*; McCleverty, J. A., Meyer, T. J., Eds.; Elsevier Pergamon, Oxford, U.K., 2004; Vol. *9*, pp 621−687. (n) Maury, O.; Le Bozec, H. *Acc. Chem. Res.* **2005**, *38*, 691. (o) Cariati, E.; Pizzotti, M.; Roberto, D.; Tessore, F.; Ugo, R. *Coord. Chem. Rev.* **2006**, *250*, 1210. (p) Coe, B. J. *Acc. Chem. Res.* **2006**, *39*, 383. (q) Zhang, C.; Song, Y.-L.; Wang, X. *Coord. Chem. Rev.* **2007**, *251*, 111.

(4) (a) Coe, B. J.; Houbrechts, S.; Asselberghs, I.; Persoons, A. *Angew. Chem., Int. Ed.* **1999**, *38*, 366. (b) Weyland, T.; Ledoux, I.; Brasselet, S.; Zyss, J.; Lapinte, C. *Organometallics* **2000**, *19*, 5235. (c) Malaun, M.; Reeves, Z. R.; Paul, R. L.; Jeffery, J. C.; McCleverty, J. A.; Ward, M. D.; Asselberghs, I.; Clays, K.; Persoons, A. *Chem. Commun.* **2001**, 49. (d) Malaun, M.; et al. *J. Chem. Soc., Dalton Trans.* **2001**, 3025. (e) Cifuentes, M. P.; Powell, C. E.; Humphrey, M. G.; Heath, G. A.; Samoc, M.; Luther-Davies, B. *J. Phys. Chem. A* **2001**, *105*, 9625. (f) Paul, F.; Costuas, K.; Ledoux, I.; Deveau, S.; Zyss, J.; Halet, J.-F.; Lapinte, C. *Organometallics* **2002**, *21*, 5229. (g) Powell, C. E.; Cifuentes, M. P.; Morrall, J. P.; Stranger, R.; Humphrey, M. G.; Samoc, M.; Luther-Davies, B.; Heath, G. A. *J. Am. Chem. Soc.* **2003**, *125*, 602. (h) Asselberghs, I.; Clays, K.; Persoons, A.; McDonagh, A. M.; Ward, M. D.; McCleverty, J. A. *Chem. Phys. Lett.* **2003**, *368*, 408. (i) Powell, C. E.; Humphrey, M. G.; Cifuentes, M. P.; Morrall, J. P.; Samoc, M.; Luther-Davies, B. *J. Phys. Chem. A* **2003**, *107*, 11264. (j) Sporer, C.; et al. *Angew. Chem., Int. Ed.* **2004**, *43*, 5266. (k) Cifuentes, M. P.; Powell, C. E.; Morrall, J. P.; McDonagh, A. M.; Lucas, N. T.; Humphrey, M. G.; Samoc, M.; Houbrechts, S.; Asselberghs, I.; Clays, K.; Persoons, A.; Isoshima, T. *J. Am. Chem. Soc.* **2006**, *128*, 10819. (l) Samoc, M.; Gauthier, N.; Cifuentes, M. P.; Paul, F.; Lapinte, C.; Humphrey, M. G. *Angew. Chem., Int. Ed.* **2006**, *45*, 7376. (m) Dalton, G. T.; Cifuentes, M. P.; Petrie, S.; Stranger, R.; Humphrey, M. G.; Samoc, M. *J. Am. Chem. Soc.* **2007**, *129*, 11882. (n) Boubekeur-Lecaque, L.; Coe, B. J.; Clays, K.; Foerier, S.; Verbiest, T.; Asselberghs, I. *J. Am. Chem. Soc.* **2008**, *130*, 3286.

(5) Coe, B. J.; Harries, J. L.; Helliwell, M.; Jones, L. A.; Asselberghs, I.; Clays, K.; Brunschwig, B. S.; Harris, J. A.; Garín, J.; Orduna, J. *J. Am. Chem. Soc.* **2006**, *128*, 12192.

(6) Selected examples: (a) Toma, H. E.; Malin, J. M. *Inorg. Chem.* **1973**, *12*, 1039. (b) Malin, J. M.; Schmidt, C. F.; Toma, H. E. *Inorg. Chem.* **1975**, *14*, 2924. (c) Toma, H. E.; Creutz, C. *Inorg. Chem.* **1977**, *16*, 545. (d) Figard, J. E.; Paukstelis, J. V.; Byrne, E. F.; Petersen, J. D. *J. Am. Chem. Soc.* **1977**, *99*, 8417. (e) Figard, J. E.; Petersen, J. D. *Inorg. Chem.* **1978**, *17*, 1059. (f) Hrepic, N. V.; Malin, J. M. *Inorg. Chem.* **1979**, *18*, 409. (g) Toma, H. E. *Can. J. Chem.* **1979**, *57*, 2079. (h) Moore, K. J.; Lee, L.-S.; Mabbott, G. A.; Petersen, J. D. *Inorg. Chem.* **1983**, *22*, 1108. (i) Johnson, C. R.; Shepherd, R. E. *Inorg. Chem.* **1983**, *22*, 1117. (j) Johnson, C. R.; Shepherd, R. E. *Inorg. Chem.* **1983**, *22*, 2439. (k) Macartney, D. H. *Rev. Inorg. Chem.* **1988**, *9*, 101–151. (l) Benedix, R.; Hennig, H. *Z. Anorg. Allg. Chem.* **1989**, *577*, 23. (m) Macartney, D. H.; Warrack, L. J. *Can. J. Chem.* **1989**, *67*, 1774. (n) Estrin, D. A.; Hamra, O. Y.; Paglieri, L.; Slep, L. D.; Olabe, J. A. *Inorg. Chem.* **1996**, *35*, 6832. (o) Slep, L. D.; Baraldo, L. M.; Olabe, J. A. *Inorg. Chem.* **1996**, *35*, 2969–6327. (p) Waldhör, E.; Kaim, W.; Olabe, J. A.; Slep, L. D.; Fiedler, J. *Inorg. Chem.* **1997**, *36*, 2969. (q) Slep, L. D.; Pollak, S.; Olabe, J. A. *Inorg. Chem.* **1999**, *38*, 4369. (r) Baraldo, L. M.; Forlano, P.; Parise, A. R.; Slep, L. D.; Olabe, J. A. *Coord. Chem. Rev.* **2001**, *219*−*221*, 881. (s) Ando, I.; Ujimoto, K.; Kurihara, H. *Bull. Chem. Soc. Jpn.* **2001**, *74*, 717. (t) Chiarella, G. M.; Melgarejo, D. Y.; Koch, S. A. *J. Am. Chem. Soc.* **2006**, *128*, 1416.

(7) Coe, B. J.; Jones, L. A.; Harris, J. A.; Brunschwig, B. S.; Asselberghs, I.; Clays, K.; Persoons, A.; Garín, J.; Orduna, J. *J. Am. Chem. Soc.* **2004**, *126*, 3880.

using either a Shimadzu UV-2401 PC or a Thermo Helios beta spectrophotometer.

Cyclic voltammetric measurements were carried out with an EG&G PAR model 283 potentiostat/galvanostat. An EG&G PAR K0264 single-compartment microcell was used with a silver/silver chloride reference electrode (3 M NaCl, saturated AgCl) separated by a salt bridge from a glassy carbon disk working electrode and Pt wire auxiliary electrode. Water and methanol were distilled before use, and KNO_3 and $[NBu^n_4]PF_6$ were used as the supporting electrolytes. Solutions containing about 10^{-3} M analyte (0.1 M electrolyte) were deaerated by purging with N_2. All $E_{1/2}$ values were calculated from $(E_{pa} + E_{pc})/2$ at a scan rate of 200 mV s^{-1}.

Synthesis of $Na_2[Fe^{II}(CN)_5(Mepyz^+)]$ (1). A solution of $[Mepyz^+]I$ (111 mg, 0.500 mmol) in water (2 mL) was added to a solution of $Na_3[Fe^{II}(CN)_5(NH_3)]$ (136 mg, 0.500 mmol) in water (4 mL), and the reaction mixture was stirred in the dark at room temperature for 16 h. The mixture was refrigerated overnight; then the solid was filtered off, washed with ethanol, and dried under vacuum. The product was purified by reprecipitation from water/ethanol to afford a dark blue solid. Yield 50 mg (28%). δ_H (D_2O) 9.73 (2 H, d, J = 4.7 Hz, $C_4H_4N_2$), 8.20 (2 H, d, J = 4.9 Hz, $C_4H_4N_2$), 4.11 (3 H, s, Me). υ(C≡N) 2095m, 2050s cm^{-1}. Anal. Calcd (%) for $C_{10}H_7N_7FeNa_2 \cdot 2H_2O$: C, 33.08; H, 3.05; N, 27.00. Found: C, 33.28; H, 2.75; N, 27.22.

Synthesis of $Na_2[Fe^{II}(CN)_5(Mebpb^+)]$ (4). A solution of $[Mebpb^+]I \cdot H_2O$ (37 mg, 0.100 mmol) in water (4 mL), with half a drop of triethylamine (TEA), was added to a solution of $Na_3[Fe^{II}(CN)_5(NH_3)]$ (29 mg, 0.107 mmol) in water (4 mL), and the reaction mixture was stirred in the dark at room temperature for 16 h. Ethanol was added until a precipitate formed; then the mixture was sonicated and refrigerated for 4 h. The dark purple/blue solid was collected by filtration, washed with ethanol, and dried. Yield 39 mg (75%). δ_H (D_2O) 8.76 (2 H, d, J = 5.7 Hz, C_5H_4N), 8.30 (2 H, d, J = 6.3 Hz, C_5H_4N), 7.72 (2 H, d, J = 6.3 Hz, C_5H_4N), 7.43 (1 H, dd, J = 11.4, 15.7 Hz, CH), 7.15 (1 H, dd, J = 11.3, 15.7 Hz, CH), 7.07 (2 H, d, J = 6.6 Hz, C_5H_4N), 6.75 (1 H, d, J = 16.7 Hz, CH), 6.73 (1 H, d, J = 16.1 Hz, CH), 4.11 (3 H, s, Me). υ(C≡N) 2085m, 2031s cm^{-1}. Anal. Calcd (%) for $C_{20}H_{15}N_7FeNa_2 \cdot 3.5H_2O$: C, 46.35; H, 4.28; N, 18.92. Found: C, 46.64; H, 3.74; N, 19.02.

Synthesis of $Na_2[Fe^{II}(CN)_5(Mebph^+)]$ (5). A solution of $[Mebph^+]Cl \cdot 2.1H_2O$ (30 mg, 0.093 mmol) in water (5 mL) was added to a solution of $Na_3[Fe^{II}(CN)_5(NH_3)]$ (28 mg, 0.103 mmol) in water (4 mL), and the reaction mixture was stirred in the dark at room temperature for 1 h. The mixture was filtered, and ethanol was added to the filtrate until a precipitate formed. After refrigeration for 3 h, the fine solid was coagulated by centrifugation for 5 min. The liquid was decanted off, and the dark blue solid washed with ethanol and dried. Yield 19 mg (38%). δ_H (D_2O) 8.68 (2 H, br s, C_5H_4N), 8.17 (2 H, d, J = 6.6 Hz, C_5H_4N), 7.61 (2 H, d, J = 6.3 Hz, C_5H_4N), 7.35 (1 H, dd, J = 12.0, 16.4 Hz, CH), 7.00−6.95 (3 H, C_5H_4N and CH), 6.72 (1 H, dd, J = 9.1, 15.5 Hz, CH), 6.61 (2 H, d, J = 15.8 Hz, CH), 6.45 (1 H, d, J = 16.1 Hz, CH), 4.03 (3 H, s, Me). υ(C≡N) 2086m, 2042s cm^{-1}. Anal. Calcd. (%) for $C_{22}H_{17}N_7FeNa_2 \cdot 5H_2O$: C, 46.25; H, 4.76; N, 17.16. Found: C, 45.73; H, 4.35; N, 18.17.

Synthesis of $Na_2[Fe^{II}(CN)_5(Mebpvb^+)]$ (6). A solution of $[Mebpvb^+]Cl \cdot H_2O$ (33 mg, 0.094 mmol) in warm water (6 mL, 40 °C) was added to a solution of $Na_3[Fe^{II}(CN)_5(NH_3)]$ (27 mg, 0.099 mmol) in water (3 mL), and the reaction mixture was stirred in the dark at room temperature for 16 h. Ethanol was added until a precipitate formed, then the mixture was sonicated and refrigerated for 4 h. The dark red solid was collected by filtration, washed with ethanol, and dried. Yield 38 mg (65%). δ_H (D_2O) 8.75 (2 H, br s, C_5H_4N), 8.14 (2 H, br s, C_5H_4N), 7.59 (2 H, br s, C_5H_4N), 7.26−7.18 (5 H, C_6H_4 and CH), 6.99−6.94 (3 H, C_5H_4N and CH), 6.77 (1 H, d, J = 14.8 Hz, CH), 6.68 (1 H, d, J = 16.7 Hz, CH), 3.90 (3 H, s, Me). υ(C≡N) 2081m, 2034s cm^{-1}. Anal. Calcd (%) for $C_{26}H_{19}N_7FeNa_2 \cdot 5H_2O$: C, 50.26; H, 4.70; N, 15.78. Found: C, 50.83; H, 4.04; N, 15.11.

Table 1. Crystallographic Data and Refinement Details for the Salts $1 \cdot 9H_2O$ and $1P \cdot 3H_2O$

	$1 \cdot 9H_2O$	$1P \cdot 3H_2O$
empirical formula	$C_{10}H_{25}FeN_7Na_2O_9$	$C_{15}H_{20}FeN_9NaO_3$
fw	489.20	453.24
appearance	blue plate	blue needle
cryst size/mm	0.25 × 0.20 × 0.04	0.15 × 0.06 × 0.03
λ/Å	0.71073	0.69260
cryst syst	monoclinic	orthorhombic
space group	$P2_1$	$Pmc2_1$
a/Å	7.9550(41)	7.6975(3)
b/Å	11.1540(19)	7.9969(3)
c/Å	12.618(2)	15.8435(6)
β/deg	97.897(3)	
U/Å^3	1109.0(3)	975.26(6)
Z	2	2
T/K	100(2)	150(2)
μ/mm^{-1}	0.772	0.834
reflns collected	9654	10119
independent reflns (R_{int})	4969 (0.0623)	3262 (0.0499)
GOF on F^2	0.763	1.097
final R1, wR2 [$I > 2\sigma(I)$][a]	0.0423, 0.0614	0.0372, 0.1040
final R1, wR2 (all data)	0.0632, 0.0659	0.0380, 0.1051

[a] The structures were refined on F_o^2 using all data; the value of R1 is given for comparison with older refinements based on F_o with a typical threshold of $F_o > 4\sigma(F_o)$.

X-ray Crystallography. Diffraction-quality crystals of the complex salt $1 \cdot 9H_2O$ were obtained via slow mixing of ethanol with an aqueous solution over about 24 h at 4 °C. Crystals of the complex salt $Na[Mepyz^+][Fe^{II}(CN)_5(Mepyz^+)] \cdot 3H_2O$ ($1P \cdot 3H_2O$) were obtained by slow diffusion of ethanol vapor into an aqueous solution over a period of about 2 weeks at 4 °C. The data for $1 \cdot 9H_2O$ were collected by using a Bruker APEX CCD X-ray diffractometer using graphite-monochromated, MoKα radiation (wavelength = 0.71073 Å). Because the crystals of $1P \cdot 3H_2O$ diffracted extremely weakly, the data in this case were collected using a wavelength of 0.6945 Å on Station 9.8 at the Synchrotron Radiation Source, Daresbury Laboratory, Warrington, Cheshire, U.K. Data processing was carried out by using the Bruker SAINT[8] software package, and a semiempirical absorption correction was applied by using SADABS.[8] The structures were solved by direct methods and refined by full-matrix least-squares on all F_0^2 data using SHELXS-97[9] and SHELXL-97.[10] All non-hydrogen atoms were refined anisotropically, with hydrogen atoms bonded to carbon or nitrogen included in calculated positions using the riding method; for $1P \cdot 3H_2O$, those bonded to the water oxygen atoms could not be located. All other calculations were carried out by using the SHELXTL package.[11] The structure of $1 \cdot 9H_2O$ comprises two complex anions in the asymmetric unit together with four Na^+ ions and eighteen water molecules. The asymmetric unit of $1P \cdot 3H_2O$ contains two complex anions with two Na^+ ions, two $Mepyz^+$ ions, and six water molecules. Crystallographic data and refinement details are presented in Table 1.

(8) *SAINT (Version 6.45) and SADABS (Version 2.10)*; Bruker AXS Inc.: Madison, WI, 2003.
(9) Sheldrick, G. M. *Acta Crystallogr., Sect. A* **1990**, *46*, 467.
(10) Sheldrick, G. M. *SHELXL 97, Program for crystal structure refinement*; University of Göttingen: Göttingen, Germany, 1997.
(11) *SHELXTL*, Version 6.10; Bruker AXS Inc.: Madison, WI, 2000.

Hyper-Rayleigh Scattering. Details of the hyper-Rayleigh scattering (HRS) experiment have been discussed elsewhere,[12] and the experimental procedure used was as previously described.[13] β values were determined by using the electric-field-induced second harmonic generation β_{1064} for *p*-nitroaniline (32.0×10^{-30} esu in methanol)[14] as an external reference. In the absence of a suitable reference for aqueous solutions, the β_{1064} values in water were obtained by using the electric-field-induced second harmonic generation β_{1064} for pNA in acetonitrile as an external reference.[14] The absolute magnitudes of these data are hence of questionable accuracy and should be compared only cautiously with the data obtained in methanol. All measurements were performed by using the 1064 nm fundamental of an injection-seeded, Q-switched Nd:YAG laser (Quanta-Ray GCR-5, 8 ns pulses, 7 mJ, 10 Hz). Dilute methanol or aqueous solutions ($10^{-5}-10^{-6}$ M) were used to ensure a linear dependence of $I_{2\omega}/I_{\omega}^2$ on solute concentration, precluding the need for Lambert−Beer correction factors. Samples were filtered (Millipore, 0.45 μm), and none showed any fluorescence. All of the sample preparation and measurements were carried out in the dark, and the solvents were degassed before use to protect the compounds from decomposition because of photoactivated ligand loss and/or aerial oxidation. One-dimensional hyperpolarizability is assumed, that is, $\beta_{1064} = \beta_{zzz}$.

Stark Spectroscopy. The Stark apparatus, experimental methods and data collection procedure were as previously reported.[5,15] The Stark spectrum for each compound was measured at least twice. The data analysis for **1** was carried out as previously described,[5,15,16] by using the zeroth, first, and second derivatives of the absorption spectrum for analysis of the Stark $\Delta\varepsilon(\nu)$ spectrum. For **4**−**6**, the absorption spectrum was modeled with three Gaussian curves, the first and second derivatives of which were used for analysis of the Stark $\Delta\varepsilon(\nu)$ spectrum in terms of the Liptay treatment.[16] The dipole moment change, $\Delta\mu_{12} = \mu_e - \mu_g$, where μ_e and μ_g are the respective excited- and ground-state dipole moments associated with each of the optical transitions considered in the fit, was then calculated from the coefficient of the second derivative component.

The Liptay equation is

$$\Delta\varepsilon(\nu)/\nu = \left[A_x\varepsilon(\nu)/\nu + \frac{B_x}{15h}\frac{\partial(\varepsilon(\nu)/\nu)}{\partial\nu} + \frac{C_x}{30h^2}\frac{\partial^2(\varepsilon(\nu)/\nu)}{\partial\nu^2}\right]\mathbf{F}_{\text{int}}^2 \quad (1)$$

where ν is the frequency of the light in Hertz and the internal electric field is related to the applied external field by $\mathbf{F}_{\text{int}} = f_{\text{int}}\mathbf{F}_{\text{ext}}$. $\Delta\mu_{12}$ is related to the coefficient of the second derivative component by

$$C_\chi = 3\Delta\mu_{12}(2 - \cos^2\chi) + 3(m\cdot\Delta\mu_{12})^2(3\cos^2\chi - 1) \quad (2)$$

where $m\cdot\Delta\mu_{12}$ is the dipole moment change along the direction of the transition dipole moment μ_{12} and χ is the angle between the polarization direction of the incident light and the applied electric field. Glycerol-water (50:50 vol %) was used as the glassing medium, for which the local field correction f_{int} is estimated as 1.33.[5,15] A two-state analysis of the intramolecular charge-transfer (ICT) transitions gives

$$\Delta\mu_{ab}^2 = \Delta\mu_{12}^2 + 4\mu_{12}^2 \quad (3)$$

where $\Delta\mu_{ab}$ is the dipole moment change between the diabatic states and $\Delta\mu_{12}$ is the observed (adiabatic) dipole moment change. The value of μ_{12} can be determined from the oscillator strength f_{os} of the transition by

$$|\mu_{12}| = [f_{os}/(1.08\times10^{-5}E_{max})]^{1/2} \quad (4)$$

where E_{max} is the energy of the ICT maximum (in wavenumbers) and μ_{12} is in Debyes. The degree of delocalization c_b^2 and electronic coupling matrix element H_{ab} for the diabatic states are given by

$$c_b^2 = \frac{1}{2}\left[1 - \left(\frac{\Delta\mu_{12}^2}{\Delta\mu_{12}^2 + 4\mu_{12}^2}\right)^{1/2}\right] \quad (5)$$

$$|H_{ab}| = \left|\frac{E_{max}(\mu_{12})}{\Delta\mu_{ab}}\right| \quad (6)$$

If the first hyperpolarizability tensor β_0 has only nonzero elements along the ICT direction, then this quantity is given by

$$\beta_0 = \frac{3\Delta\mu_{12}(\mu_{12})^2}{(E_{max})^2} \quad (7)$$

A relative error of ±20−30% is estimated for the β_0 values derived from the Stark data and using eq 7, while experimental errors of ±10−15% are estimated for μ_{12} and $\Delta\mu_{12}$, ±40% for $\Delta\mu_{ab}$, ±30% for H_{ab}, and ±50% for c_b^2 when the Stark spectra can be fit with the experimentally observed spectra.

Results and Discussion

Synthetic Studies. We have previously reported the syntheses of a series of $\{Fe^{II}(CN)_5\}^{3-}$-based complex salts, including **2** and **3**.[5] The $Mepyz^+$ complex in **1** has been studied on a number of previous occasions[6] but without any structural characterization. The new complex salts **4**−**6** (Figure 1) were prepared simply by substitution of the ammine ligand in the commercially available precursor $Na_3[Fe^{II}(CN)_5(NH_3)]$. A reaction time of 16 h at room temperature gave good yields for **1**, **4**, and **6**, but in the case of **5** a satisfactorily pure product could not be isolated by using this approach. Using a much shorter reaction time of only 1 h did afford **5** in pure form, but with a rather lower isolated yield. Salts **2** and **3** were prepared previously by using an intermediate reaction time of 6 h.[5]

The new compounds give diagnostic ^{1}H NMR spectra attributable to the pyridyl ligands, and the lack of any other signals confirms the absence of uncoordinated pyridyl species or multisubstituted complexes. The chemical shifts measured for salt **1** are similar to those previously determined using a

(12) (a) Clays, K; Persoons, A. *Phys. Rev. Lett.* **1991**, *66*, 2980. (b) Clays, K.; Persoons, A. *Rev. Sci. Instrum.* **1992**, *63*, 3285. (c) Hendrickx, E.; Clays, K.; Persoons, A.; Dehu, C.; Brédas, J.-L. *J. Am. Chem. Soc.* **1995**, *117*, 3547. (d) Hendrickx, E.; Clays, K.; Persoons, A. *Acc. Chem. Res.* **1998**, *31*, 675.
(13) Houbrechts, S.; Clays, K.; Persoons, A.; Pikramenou, Z.; Lehn, J.-M. *Chem. Phys. Lett.* **1996**, *258*, 485.
(14) Stähelin, M.; Burland, D. M.; Rice, J. E. *Chem. Phys. Lett.* **1992**, *191*, 245.
(15) (a) Shin, Y.-g. K.; Brunschwig, B. S.; Creutz, C.; Sutin, N. *J. Phys. Chem.* **1996**, *100*, 8157. (b) Coe, B. J.; Harris, J. A.; Brunschwig, B. S. *J. Phys. Chem. A* **2002**, *106*, 897.
(16) (a) Liptay, W. In *Excited States*; Lim, E. C., Ed.; Academic Press: New York, 1974; Vol. 1, pp 129−229. (b) Bublitz, G. U.; Boxer, S. G. *Annu. Rev. Phys. Chem.* **1997**, *48*, 213. (c) Brunschwig, B. S.; Creutz, C.; Sutin, N. *Coord. Chem. Rev.* **1998**, *177*, 61.

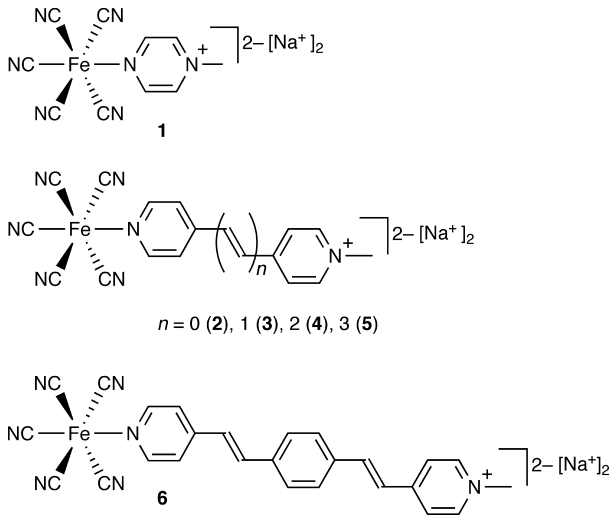

Figure 1. Chemical structures of the Fe^{II} complex salts investigated.

Table 2. UV–vis Absorption and Electrochemical Data for **1**−**6** in Water

salt (L)	λ_{max}, nm (ε, 10^3 M^{-1} cm^{-1})[a]	E_{max} (eV)[a]	assignment	E, V vs Ag/AgCl (ΔE_p, mV)[b] $E_{1/2}[Fe^{III/II}]$	$E_{1/2}$ or E_{pc}[c]
1 ($Mepyz^+$)	661 (9.5)	1.88	d → π*	0.76 (75)	−0.65 (85)
	277 (5.2)	4.48	π → π*		
2 (MeQ^+)[d]	531 (5.3)	2.34	d → π*	0.48 (190)	−0.90 (320)
	263 (22.9)	4.71	π → π*		−1.42
3 ($Mebpe^+$)[d]	533 (5.7)	2.33	d → π*	0.45 (130)	−0.94
	314 (30.8)	3.95	π → π*		
	226 (19.4)	5.49	π → π*		
4 ($Mebpb^+$)	521 (7.3)	2.38	d → π*	0.43 (120)	−0.87
	354 (46.6)	3.50	π → π*		
5 ($Mebph^+$)	496 (6.1)	2.50	d → π*	0.41 (125)	−0.87
	384 (41.1)	3.23	π → π*		
6 ($Mebpvb^+$)	467 (8.0)	2.66	d → π*	0.39 (95)	−0.98
	377 (56.0)	3.29	π → π*		

[a] Solutions about 3−8 × 10^{-5} M. [b] Solutions about 10^{-3} M in 0.1 M aqueous KNO_3 at a glassy carbon disk working electrode with a scan rate of 200 mV s^{-1}. [c] For an irreversible reduction process. [d] Data taken in part from ref 5.

60 MHz machine.[6b] Although the fits are not always optimal, CHN elemental analyses provide further evidence for the expected identity and purity of the products. These measurements confirm the presence of substantial amounts of water of crystallization, consistent with the hygroscopic nature of such salts as documented in previous investigations with related compounds[6a,d,17] and verified by TGA.[18]

Electronic Spectroscopy Studies. The UV−vis absorption spectra of complex salts **1** and **4**−**6** have been measured in both water and methanol, and the results are shown in Tables 2 and 3, together with the corresponding data for **2** and **3** for comparison purposes.[5] Representative spectra of salts **1** and **4** are shown in Figure 2. These spectra feature intense UV absorptions due to $\pi \rightarrow \pi^*$ intraligand transitions that are expected to display significant charge-transfer (ILCT) character in the extended chromophores, together with intense

(17) Alborés, P.; Slep, L. D.; Weyhermüller, T.; Baraldo, L. M. *Inorg. Chem.* **2004**, *43*, 6762.

(18) The extent of agreement between the results of the TGA and elemental analyses is variable, but generally reasonable, for example, for compound **4** TGA indicates the loss of about 2.8 molecules of water upon heating while the CHN analyses fit quite well to 3.5 molecules.

Table 3. UV–vis Absorption and Electrochemical Data for **1**−**6** in Methanol

salt (L)	λ_{max}, nm (ε,10^3 M^{-1} cm^{-1})[a]	E_{max} (eV)[a]	assignment	E, V vs Ag/AgCl (ΔE_p, mV)[b] $E_{1/2}[Fe^{III/II}]$	$E_{1/2}$ or E_{pc}[c]
1 ($Mepyz^+$)	729 (9.7)	1.70	d → π*	0.63 (85)	−0.64 (95)
	280 (4.3)	4.43	π → π*		
2 (MeQ^+)[d]	681 (5.6)	1.82	d → π*	0.28 (130)	−0.72 (140)
	271 (18.0)	4.58	π → π*		
3 ($Mebpe^+$)[d]	685 (5.5)	1.81	d → π*	0.24 (150)	−0.60
	319 (29.0)	3.89	π → π*		
	229 (17.6)	5.41	π → π*		
4 ($Mebpb^+$)	654 (7.6)	1.90	d → π*	0.21 (90)	−0.63
	357 (50.0)	3.47	π → π*		
5 ($Mebph^+$)	590 (7.0)	2.10	d → π*	0.20 (95)	−0.67
	387 (52.0)	3.20	π → π*		
6 ($Mebpvb^+$)	561 (7.4)	2.21	d → π*	0.19 (80)	−0.66
	383 (57.8)	3.24	π → π*		

[a] Solutions about 3−8 × 10^{-5} M. [b] Solutions about 10^{-3} M in 0.1 M $[NBu^n_4]PF_6$ in methanol at a glassy carbon disk working electrode with a scan rate of 200 mV s^{-1}. Ferrocene internal reference $E_{1/2}$ = 0.67 V, ΔE_p = 80−130 mV. [c] For an irreversible reduction process. [d] Data taken in part from ref 5.

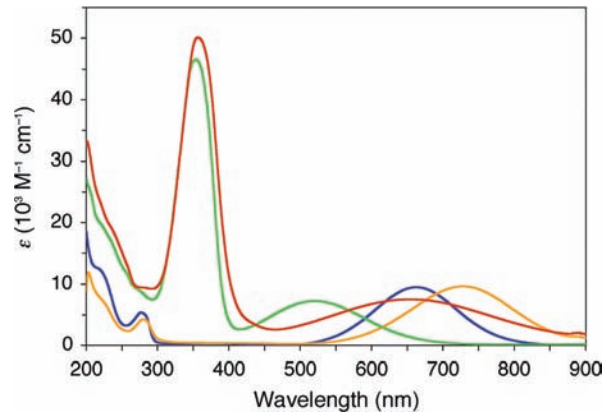

Figure 2. UV−vis absorption spectra of **1** in water (blue) and methanol (gold) and **4** in water (green) and methanol (red) at 293 K.

and very broad $d(Fe^{II}) \rightarrow \pi^*(L)$ (L = $Mepyz^+$/pyridyl ligand) visible MLCT bands. Because the latter are not very well defined, the quoted λ_{max} and E_{max} values should be treated as estimates with substantial error limits.

As noted previously,[5] dipolar $\{Fe^{II}(CN)_5\}^{3-}$ complexes are strongly solvatochromic because of marked interactions between the cyanide ligands and the solvent medium. The isolated Na^+ salts do not dissolve appreciably in most common organic solvents, but are highly soluble in water and methanol. The MLCT bands of the salts **2**−**6** show large red-shifts of about 0.4−0.5 eV on moving from water to methanol (Tables 2 and 3, Figure 2), but a smaller corresponding shift of about 0.2 eV is observed for **1**. The lower degree of solvatochromism shown by the complex in **1** is a logical and predictable consequence of its smaller value of $\Delta\mu_{12}$ when compared with the extended species (see below, Table 6). These decreases in the MLCT E_{max} are attributable to increases in the electron density at the Fe^{II} center, primarily because of the weaker H-bond donating ability of methanol versus water. A lesser extent of H-bonding with the solvent increases the basicity and decreases the π-accepting ability of the cyanide ligands. The energies of the intraligand transitions are almost insensitive to changing the solvent

because of their confinement within the ligand π-framework and less directional nature when compared with the MLCT processes. The molar extinction coefficients generally show relatively small variations on changing the solvent, and no trend is evident.

The electronic absorption data for **1** in aqueous solution (Table 2) are similar to those reported previously, except that the MLCT intensity we find is substantially smaller. The original value of 12.0×10^3 M^{-1} cm^{-1} quoted by Toma and Malin[6a] has been assumed correct in a number of subsequent studies, and Figard et al. have claimed an even larger value of 14.0×10^3 M^{-1} cm^{-1}.[6d] However, we have recorded spectra on a number of different samples that were carefully purified and assessed by using both high-field ^1H NMR spectroscopy and CHN analyses, with protection from light and air, and have been unable to duplicate these earlier results. It is also worth noting that the MLCT ε value for **1** in water is not appreciably concentration dependent, varying by only as much as 3% over the range $1.41 \times 10^{-4}-1.41 \times 10^{-5}$ M. These observations rule out any aggregation effects as the cause of the disagreement with reported data. We are hence confident that our results are reliable, and this conclusion has implications for a number of previous quantitative spectroscopic, kinetic, and other studies involving the complex in **1**. Given this fact, it is quite remarkable that so many reports have simply assumed the originally published ε value to be correct, without actually attempting to reproduce it. It is, however, notable that Slep et al. have estimated a relatively low MLCT ε value of 6.9×10^3 M^{-1} cm^{-1} for the closely related complex $[Fe^{II}(CN)_5(Hpyz^+)]^{2-}$ ($\lambda_{max} = 636$ nm in aqueous HCl).[6q] Interestingly, the MLCT ε value we find for compound **2** is only slightly smaller than that reported by Toma and Malin (5.6×10^3 M^{-1} cm^{-1}),[6a] while Macartney and Warrack's MLCT ε value for compound **3** (6.9×10^3 M^{-1} cm^{-1})[6m] is also somewhat larger than that which we have determined (Table 2). Despite the discrepancy when compared with the previous literature, **1** still displays the most intense MLCT absorption among the complexes studied here.

In water, the MLCT energy of **1** is considerably lower than those of **2**−**6**; the MLCT band is red-shifted by about 0.5 eV when compared with that for **3** and by about 0.8 eV when compared with that for **6** (Table 2). The same pattern is evident in methanol (Table 3), but the decrease in E_{max} on moving from **1** to its extended congeners covers a smaller range of about 0.1−0.5 eV. Moving from the MeQ^+ complex salt **2** to its $Mebpe^+$ analogue **3** produces only very slight red-shifts in the MLCT absorption maxima, together with small intensity changes.[5] However, the addition of further *E*-ethylene units leads to blue-shifts in the MLCT band that increase going along the series in both solvents (Tables 2 and 3). Thus, moving from the $Mebpe^+$ complex salt to **4** increases E_{max} by 0.05 and 0.09 eV in water and methanol, respectively, and larger corresponding increases of 0.12 and 0.20 eV are observed between **4** and **5**. The MLCT ε values increase on moving from **3** to **4**, then decrease in **5**. A similar, relatively unusual trend of blue-shifting of the MLCT band with extending conjugation is also observed in the analogous $\{Ru^{II}(NH_3)_5\}^{2+}$ and *trans*-$\{Ru^{II}Cl(pdma)_2\}^+$ [pdma = 1,2-phenylenebis(dimethylarsine)] complexes.[7,19] In contrast, the ILCT transitions show red-shifts as the chromophore length increases within the series **2**−**5**, generally accompanied by increases in intensity, while small blue-shifts and ε increases are observed on moving from **5** to **6**. Again, these patterns parallel those found in the related $\{Ru^{II}(NH_3)_5\}^{2+}$- and *trans*-$\{Ru^{II}Cl(pdma)_2\}^+$-based complexes,[7,19] and the ILCT band energies are essentially independent of the nature of the coordinated metal center. Replacing an ethylene with a 1,4-phenylene group in moving from **5** to **6** causes MLCT blue shifts of 0.16 and 0.11 eV in water and methanol, respectively, with the MLCT band beginning to overlap with the ILCT band in water. Corresponding blue shifts have been reported previously for the analogous Ru^{II} ammine/pdma complexes containing bph/bpvb units.[7,19]

Electrochemical Studies. The complex salts **1** and **4**−**6** were studied by cyclic voltammetry in both water and methanol, and the results are presented in Tables 2 and 3, together with the corresponding data for **2** and **3** for comparison purposes.[5] In all cases, reversible or quasi-reversible $Fe^{III/II}$ waves are observed, together with a reversible ligand-based reduction process for **1** and an irreversible ligand-based process for **4**−**6**. For **1**, the close similarity in the peak current magnitudes between the latter and the $Fe^{III/II}$ waves indicates one-electron processes corresponding with the $Mepyz^+/Mepyz^\bullet$ couple.

Toma and Creutz previously determined a $E_{1/2}[Fe^{III/II}]$ value of 0.79 V versus SCE for **1** measured in 1 M aqueous NaCl buffered at pH 4.5 with a platinum working electrode, but did not comment on the reductive behavior.[6c] Waldhör et al. reported a $E_{1/2}[Fe^{III/II}]$ value of 0.63 V versus Ag/AgCl for **1** measured in 0.1 M aqueous KCl buffered at pH 7 with a glassy carbon working electrode, but the accompanying ligand-based reduction at −0.70 V was irreversible.[6p] In unbuffered 0.1 M aqueous KNO_3 at a glassy carbon electrode, our measured $E_{1/2}[Fe^{III/II}]$ lies in between these reported values (Table 2). Within the extended *N*-methylpyridinium series, the sequential addition of *E*-ethylene units to the pyridyl ligands makes the Fe^{II} center slightly easier to oxidize; in water (Table 2), the $E_{1/2}[Fe^{III/II}]$ value decreases by 30 mV on moving from the MeQ^+ complex in **2** to its $Mebpe^+$ counterpart in **3**, and by further successive 20 mV increments on proceeding to **4** and then **5**. A further decrease of 20 mV is observed on moving from **5** to **6**, on replacement of the central *E* ethylene bond with a 1,4-phenylene unit. The $E_{1/2}[Fe^{III/II}]$ data recorded in methanol (Table 3) show the same trend as observed in water, but the differences between the potentials for **4**−**6** are smaller.

As noted previously for **2** and **3** and related compounds,[5] the $E_{1/2}[Fe^{III/II}]$ values for **4**−**6** decrease by about 200 mV on moving from water to methanol. These observations indicate substantial relative destabilization of the Fe-based

(19) (a) Coe, B. J.; Harries, J. L.; Harris, J. A.; Brunschwig, B. S.; Coles, S. J.; Light, M. E.; Hursthouse, M. B. *Dalton Trans.* **2004**, 2935. (b) Coe, B. J.; Harries, J. L.; Harris, J. A.; Brunschwig, B. S.; Horton, P. N.; Hursthouse, M. B. *Inorg. Chem.* **2006**, *45*, 11019.

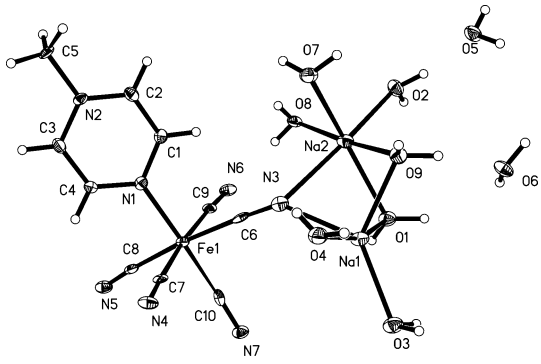

Figure 3. Representation of the molecular structure of **1**·9H_2O (50% probability ellipsoids).

highest occupied molecular orbitals (HOMOs) in methanol, attributable to the differing solvent−solute interactions that also affect the MLCT energies (see above). The smaller decrease in $E_{1/2}$[$Fe^{III/II}$] of about 130 mV observed for **1** on moving from water to methanol is consistent with the fact that this compound also shows a corresponding solvatochromic red-shift that is about half as large as those found for **2**−**6**.

In water, the $Mepyz^+$/$Mepyz^{\bullet}$ wave for **1** occurs at a potential somewhat higher than those of the ligand-based processes in **2**−**6** (Table 2), but in methanol this situation no longer applies (Table 3) because while the reduction waves for **2**−**6** shift to higher potentials, the $Mepyz^+$/$Mepyz^{\bullet}$ process is not affected by changing the solvent. Thus the difference between the $Fe^{III/II}$ and $Mepyz^+$/$Mepyz^{\bullet}$ waves for **1** decreases by about 140 mV on moving from water to methanol. It is noteworthy that although the potential separation between the first oxidation and reduction processes is larger for **1** when compared with **2** in both solvents, the $Mepyz^+$ complex still has the lowest MLCT energy.

Crystallographic Studies. Single crystal X-ray structures have been obtained for the complex salts **1**·9H_2O and Na[$Mepyz^+$][$Fe^{II}(CN)_5(Mepyz^+)$]·3H_2O (**1P**·3H_2O). The latter material was obtained from a crystallization carried out on an extended time scale and is evidently a decomposition product of **1** in which some of the $Mepyz^+$ has dissociated from the iron center. This result is not surprising given that the Fe−N bonds in such complexes are relatively susceptible to both photochemical and thermal cleavage. Representations of the molecular structures of **1**·9H_2O and **1P**·3H_2O are shown in Figures 3 and 4, and selected interatomic distances and angles are presented in Table 4. To our knowledge, the only previously reported structures of compounds containing a $\{Fe^{II}(CN)_5\}^{3-}$ unit coordinated to a pyridyl ligand are the salts **2**·9H_2O[5] and $[Et_4N]_3[Fe^{II}(CN)_5(py)]$ (py = pyridine).[6t]

Both structures show the expected octahedrally coordinated Fe^{II} ion, and in each case the Fe−C bond located trans to the $Mepyz^+$ ligand is shorter by 0.04−0.03 Å when compared with the other four Fe−C bonds (Table 4). This observation can be attributed to the relative structural trans effects of the cyanide and $Mepyz^+$ ligands;[20] the mutually trans Fe−C bonds are probably weakened because of the relatively strong σ-donating ability of CN^-, and it may also

(20) Coe, B. J.; Glenwright, S. J. *Coord. Chem. Rev.* **2000**, *203*, 5.

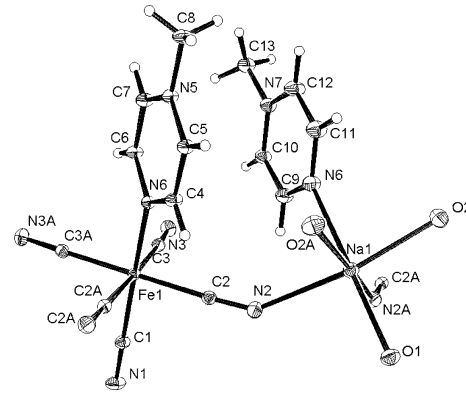

Figure 4. Representation of the molecular structure of **1P**·3H_2O (50% probability ellipsoids). The protons on the coordinated water molecules are not shown because they were not located crystallographically.

Table 4. Selected Interatomic Distances (Å) and Angles (deg) for the Salts **1**·9H_2O and **1P**·3H_2O

	1·9H_2O	**1P**·3H_2O
Fe−C(trans N)	1.878(4)	1.905(3)
Fe−C(trans C)	1.915(4)[a]	1.9242(19)
Fe−C(trans C)	1.929(4)	1.9242(19)
Fe−C(trans C)	1.915(4)	1.9377(18)
Fe−C(trans C)	1.925(4)	1.9377(18)
Fe−N	1.971(3)	1.960(2)
N−C(H)	1.356(4)	1.351(3)
N−C(H)	1.335(4)	1.356(3)
C(H)−C(H)	1.373(5)	1.378(3)
C(H)−C(H)	1.387(5)	1.379(3)
C(H)−N	1.335(4)	1.340(3)
C(H)−N	1.339(4)	1.351(4)
N−CH_3	1.481(4)	1.483(3)
N−Fe−C(trans N)	178.03(16)	177.86(10)
N−Fe−C(trans C)	93.15(13)	92.32(7)
N−Fe−C(trans C)	92.10(14)	92.32(7)
N−Fe−C(trans C)	92.19(14)	88.59(7)
N−Fe−C(trans C)	90.43(14)	88.59(7)
C(trans C)−Fe−C(trans N)	88.15(15)	89.24(8)
C(trans C)−Fe−C(trans N)	88.13(16)	89.24(8)
C(trans C)−Fe−C(trans N)	86.63(16)	89.90(7)
C(trans C)−Fe−C(trans N)	89.37(16)	89.90(7)
C(trans C)−Fe−C(trans C)	88.69(15)	90.02(10)
C(trans C)−Fe−C(trans C)	174.58(16)	177.63(8)
C(trans C)−Fe−C(trans C)	85.57(15)	85.60(11)
C(trans C)−Fe−C(trans C)	92.64(16)	92.19(7)
C(trans C)−Fe−C(trans C)	173.81(17)	177.63(8)
C(trans C)−Fe−C(trans C)	92.86(16)	92.19(7)

[a] CN^- ligand also coordinated to two Na^+ cations.

be the case that this ligand competes more effectively for π-electron density than does $Mepyz^+$. Even so, the Fe−N($Mepyz^+$) distances are relatively short (1.971(3) and 1.960(2) Å for **1**·9H_2O and **1P**·3H_2O, respectively), indicating that extensive π-back-bonding to this ligand is present. It is noteworthy that these two distances are significantly different, the relatively shorter bond length in **1P**·3H_2O suggesting a greater degree of π-back-bonding to $Mepyz^+$. The Fe−C distance to the trans CN^- ligand is also longer by about 0.03 Å in **1P**·3H_2O when compared with **1**·9H_2O (Table 4); this observation correlates with the change in the Fe−N($Mepyz^+$) distances because the mutually trans ligands are competing for π-electron density from Fe^{II}, so less π-back-bonding to the trans CN^- ligand occurs in **1P**·3H_2O, giving a relatively longer Fe−C bond. Although it is thus clear that crystal packing factors can significantly influence

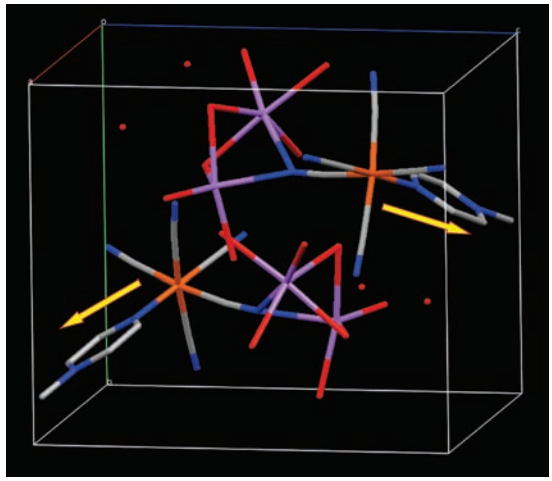

Figure 5. Crystal packing diagram of **1**·9H_2O, viewed approximately perpendicular to the 2-fold screw (*b*) axis (H atoms removed for clarity). The arrows approximate to the directions of the molecular dipolar axes.

the electronic structure of the $[Fe^{II}(CN)_5(Mepyz^+)]^{2-}$ complex anion, we are unable to explain the observed differences in terms of specific interactions with the surrounding ions or water molecules. The Fe−N(MeQ^+) distance in **2**·9H_2O is 2.026(1),[5] about 0.06 Å longer than the Fe−N($Mepyz^+$) distances in **1**·9H_2O and **1P**·3H_2O, while the Fe−N(py) distance in $[Et_4N]_3[Fe^{II}(CN)_5(py)]$ is longer still at 2.039(4).[6t] This trend can be ascribed to the relatively weaker π-acceptor ability of the MeQ^+ and py ligands when compared with $Mepyz^+$. The structure of $[Ru^{II}(NH_3)_5(Mepyz^+)]I_3$ also contains an unusually short metal-N($Mepyz^+$) bond, again attributable to strong π-back-bonding interactions.[21]

In the structure of **1**·9H_2O, one of the Na^+ cations is terminally coordinated to three H_2O molecules, while the other Na^+ has only two such terminal ligands and the two cations are bridged by two further H_2O molecules. Two additional H_2O molecules are present but uncoordinated (Figure 3). The Na^+ ions are also coordinated to the N atom of one of the equatorial CN^- ligands, so that one Na^+ has a pseudo-octahedral coordination geometry while the other is pseudotrigonal bipyramidally coordinated. The Fe−C distance is not significantly affected by the coordination of its connected N atom to Na^+ (Table 4). The salt **1P**·3H_2O displays a polymeric packing arrangement, with each Na^+ octahedrally coordinated to two N atoms of equatorial CN^- ligands and a $Mepyz^+$ ligand, with three H_2O molecules in a facial arrangement (Figure 4). The structures of both **1**·9H_2O and **1P**·3H_2O feature extensive hydrogen bonding interactions between the H_2O molecules and the CN^- ligands.

The salts **1**·9H_2O and **1P**·3H_2O adopt the non-centrosymmetric space groups $P2_1$ and $Pmc2_1$, respectively, potentially allowing bulk quadratic NLO effects to be observed. However, the crystal packing structures involve quite different relative orientations of the individual dipolar $[Fe^{II}(CN)_5(Mepyz^+)]^{2-}$ units (Figures 5 and 6), meaning that differing $\chi^{(2)}$ values can be expected for these two materials. In **1**·9H_2O, the 2-fold screw (*b*) axis is perpendicular to the *ac* plane and forms an angle of 66.99° with the dipolar

(21) Wishart, J. F.; Bino, A.; Taube, H. *Inorg. Chem.* **1986**, *25*, 3318.

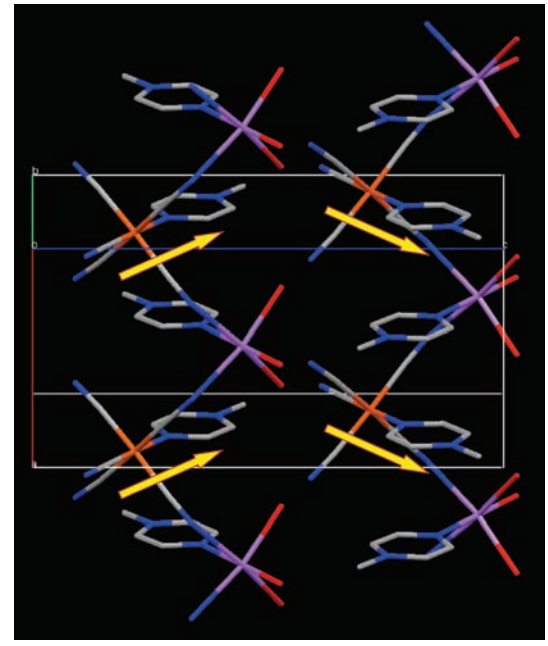

Figure 6. Crystal packing diagram of **1P**·3H_2O, viewed approximately perpendicular to the 2-fold symmetry (*a*) axis (H atoms removed for clarity). The arrows approximate to the directions of a the molecular dipolar axes.

Fe−N−N($Mepyz^+$) axis of the complexes (approximated as corresponding with the Fe−N2 vector) (Figure 5). In contrast, in **1P**·3H_2O, the $[Fe^{II}(CN)(Mepyz^+)]^{2+}$ units lie in the *bc* plane, and their dipoles form an angle of 54.47° with the *c* axis (Figure 6). The $[Na(CN)(Mepyz^+)]^+$ units are parallel with their Fe^{II} counterparts, and the two types of complex are interleaved. When compared with **1**·9H_2O, the chromophore density is decreased for **1P**·3H_2O because of the presence of the Na^+-coordinated $Mepyz^+$ ligands.

Hyper-Rayleigh Scattering Studies. Complex salts **1** and **4**−**6** were studied in both water and methanol by using the HRS technique[12,13] with a 1064 nm Nd:YAG laser fundamental. Values of β_0 were obtained by using the two-state model,[22] and the results are presented in Table 5, together with the corresponding data for **2** and **3** for comparison purposes.[5] It is worth noting that the intense ILCT bands are likely to contribute significantly to the NLO responses of the extended chromophores in **4**−**6**,[7,19b] but only the MLCT transitions are considered here because such low energy excitations are expected to be dominant.

The β_0 values obtained for the newly studied complexes in both solvents are relatively large, but no clear trend is observed when comparing the data obtained in methanol with those in water, despite the consistent and marked accompanying red-shifts of the MLCT transitions. When considering its molecular length and the data for the analogous extended chromophores, **1** shows relatively large β_0 responses. Because our previous investigations with analogous $\{Ru^{II}(NH_3)_5\}^{2+}$ complexes have revealed an unusual maximization of β_0 in *E*,*E*-buta-1,3-dienyl-bridged chromophores,[7] the conjugation length dependence of the

(22) (a) Oudar, J. L.; Chemla, D. S. *J. Chem. Phys.* **1977**, *66*, 2664. (b) Oudar, J. L. *J. Chem. Phys.* **1977**, *67*, 446.

Table 5. MLCT Absorption and HRS Data for **1**−**6**

	water			methanol		
salt (L)	λ_{max} (nm)	β_{1064}[a] (10^{-30} esu)	β_0[b] (10^{-30} esu)	λ_{max} (nm)	β_{1064}[a] (10^{-30} esu)	β_0[b] (10^{-30} esu)
1 (Mepyz$^+$)	660	500 ± 40	165 ± 14	728	269 ± 25	125 ± 11
2 (MeQ$^+$)[c]	534	311 ± 47	2 ± 0.3[d]	686	330 ± 50	128 ± 19
3 (Mebpe$^+$)[c]	538	239 ± 36	4 ± 0.6[d]	685	363 ± 54	140 ± 21
4 (Mebpb$^+$)	520	2160 ± 408	73 ± 14[d]	654	664 ± 86	211 ± 27
5 (Mebph$^+$)	502	665 ± 167	56 ± 14	614	1798 ± 335	398 ± 74
6 (Mebpvb$^+$)	465	1194 ± 280	228 ± 54	561	761 ± 196	61 ± 15[d]

[a] From 1064 nm HRS measurements at 295 K. [b] Derived from β_{1064} by using the two-state model.[22] [c] Data taken from ref 5. [d] Underestimated due to proximity of λ_{max} to 532 nm.

Table 6. MLCT Absorption and Stark Spectroscopic Data for **1**−**6**[a]

salt (L)	λ_{max} (nm)	E_{max} (eV)	f_{os}[b]	μ_{12}[c] (D)	$\Delta\mu_{12}$[d] (D)	$\Delta\mu_{ab}$[e] (D)	r_{12}[f] (Å)	r_{ab}[g] (Å)	c_b^2[h]	H_{ab}[i] (10^3 cm^{-1})	β_0[j] (10^{-30} esu)
1 (Mepyz$^+$)	649	1.91	0.14	4.4	7.3	11.4	1.5	2.4	0.18	6.0	45
2 (MeQ$^+$)[k]	533	2.33	0.11	3.5	22.5	23.6	4.7	4.9	0.02	2.8	61
3 (Mebpe$^+$)[k]	557	2.23	0.16	4.4	25.9	27.4	5.4	5.7	0.03	2.9	119
4 (Mebpb$^+$)	585	2.12	0.03	2.0	26.6	26.9	5.6	5.6	0.01	1.3	27
	521	2.38	0.11	3.5	22.1	23.2	4.6	4.8	0.02	2.9	54
5 (Mebph$^+$)	580	2.14	0.02	1.7	34.6	34.7	7.2	7.2	0.00	0.8	24
	519	2.39	0.10	3.3	26.6	27.5	5.6	5.7	0.02	2.3	59
6 (Mebpvb$^+$)	531	2.33	0.07	2.7	35.3	35.7	7.4	7.4	0.01	1.4	56
	486	2.55	0.10	3.2	28.3	28.9	5.9	6.0	0.01	2.2	50

[a] In glycerol-water (50:50 vol %) glasses at 77 K. [b] For **1**−**3**, obtained from $(4.32 \times 10^{-9}$ M cm$^2)A$ where A is the numerically integrated area under the absorption peak; for the spectra treated by using Gaussian fitting (salts **4**−**6**), obtained from $(4.60 \times 10^{-9}$ M cm$^2)\varepsilon_{max} \times fw_{1/2}$ where ε_{max} is the maximal molar extinction coefficient and $fw_{1/2}$ is the full width at half-height (in wavenumbers). [c] Calculated from eq 4. [d] Calculated from $f_{int}\Delta\mu_{12}$ by using $f_{int} = 1.33$. [e] Calculated from eq 3. [f] Delocalized electron-transfer distance calculated from $\Delta\mu_{12}/e$. [g] Effective (localized) electron-transfer distance calculated from $\Delta\mu_{ab}/e$. [h] Calculated from eq 5. [i] Calculated from eq 6. [j] Calculated from eq 7. [k] Data taken from ref 5.

NLO responses in the series **2**−**5** is of interest. As n changes from 2 to 3 (i.e., moving from **4** to **5**), the measurements in water and methanol show conflicting trends, but the β_0 value obtained for **5** in methanol is in any case rather larger than anticipated. Although the complex salt **6** displays the largest β_0 value of all the compounds studied in water, this situation is reversed in methanol; this effect can be attributed largely to the proximity of the MLCT band to the second harmonic wavelength in the latter solvent. Because of severe underestimation of β_0 for the related Mebpe$^+$ complex in water,[5] comparison across the complete *N*-methylated series in this solvent is not possible. However, in methanol, β_0 increases steadily on moving from $n = 0$ to 3. This trend follows that observed in the analogous $\{Ru^{II}(NH_3)_5\}^{2+}$ complexes, except that the latter show a substantial decrease in NLO response on moving from $n = 2$ to 3.

The observation of considerably larger β_0 values for **4** and **5** when compared with **3** in methanol provides a notable contrast with the Stark results which show an opposite pattern (see below). However, it should be noted that the UV−vis and electrochemical data show that the different conditions under which the Stark and HRS data were obtained can be expected to influence dramatically the molecular electronic/optical properties of the compounds studied. In addition, the HRS experiments probe the overall NLO responses, while the Stark analyses are limited to those associated with the MLCT transitions.

Stark Spectroscopic Studies. We have studied complex salts **1** and **4**−**6** by using Stark spectroscopy on the MLCT bands in glycerol-water (50:50 vol %) glasses at 77 K, and the results are shown in Table 6, together with the corresponding data for **2** and **3** for comparison purposes.[5] Representative absorption and electroabsorption spectra for **4**−**6** are shown in Figure 7.

Complex salt **1** proved straightforward to analyze, but deconvolution of the absorption spectra using three Gaussian functions was necessary for compounds **4**−**6** to give acceptable data fits. In these analyses, one high energy function was used to model the ILCT band, while two Gaussian curves were necessary to fit the MLCT band, with significant overlap between the two bands. Our previous studies with the corresponding $\{Ru^{II}(NH_3)_5\}^{2+}$ and *trans*-$\{Ru^{II}Cl(pdma)_2\}^+$ complexes have shown that the intense ILCT bands also contribute significantly to the NLO responses of extended chromophores such as those in **4**−**6**.[7,19] However, it was not possible to obtain accurate fits for the high energy functions for **4**−**6** (Figure 7) because of instrumental limitations, so the following discussion focuses solely on the MLCT bands. Assuming that all of the observed visible absorption arises from MLCT transitions, even if the band is divided into two or more components, then each of these can be adequately described by a two-state model (comprising a ground and one excited state). In other related studies,[23] we have found that using such an approach generally leads to total β_0 values that are similar to those derived without any spectral deconvolution.

On moving from **1** to **2**, f_{os} and μ_{12} both decrease, but $\Delta\mu_{12}$ and $\Delta\mu_{ab}$ increase dramatically because of the increased chromophore length. The corresponding electron-transfer distances also increase 2−3-fold. For **1**, the values of c_b^2 and H_{ab} are relatively large, indicating the presence of extensive π-orbital overlap and electronic coupling that is logically much more significant when compared with the extended chromophores in **2**−**6**. Within the series **2**−**5**, as the π-conjugation is extended, the values of f_{os} and μ_{12} show

(23) Coe, B. J.; Foxon, S. P.; Harper, E. C.; Harris, J. A.; Helliwell, M.; Raftery, J.; Asselberghs, I.; Clays, K.; Franz, E.; Brunschwig, B. S.; Fitch, A. G. *Dyes Pigm.*, **2009**, *81*, in press.

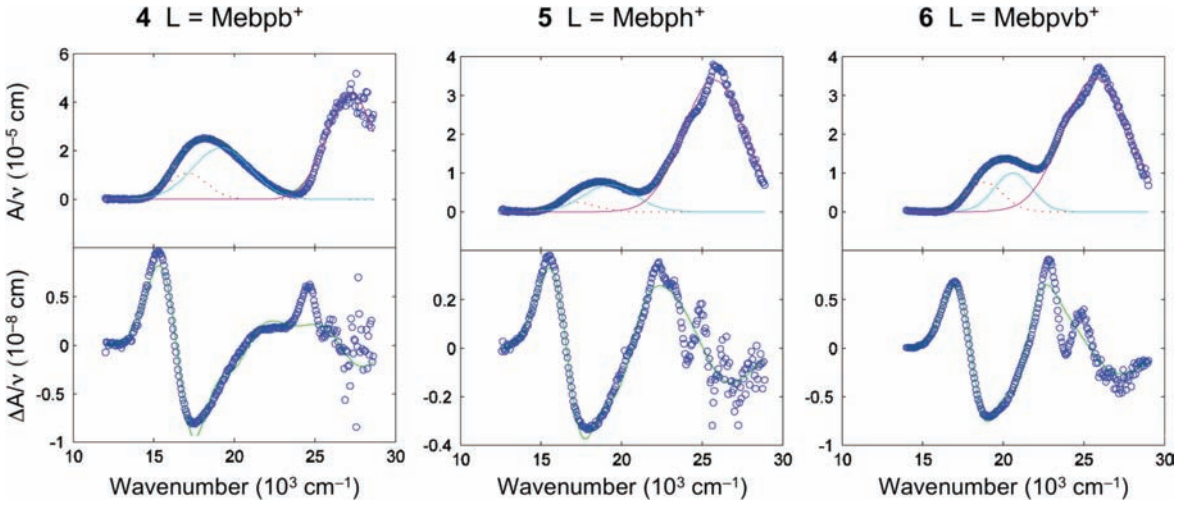

Figure 7. Absorption and electroabsorption spectra and calculated fits for complex salts **4**−**6** in an external field of 1.9×10^7 V m^{-1}. Top panels: absorption spectra illustrating the three Gaussian curves used in the data fitting (blue = experimental); bottom panels: electroabsorption spectra (blue = experimental, green = fit) according to eq 1.[16]

no clear trend, but $\Delta\mu_{12}$, $\Delta\mu_{ab}$, r_{12}, and r_{ab} clearly increase with the conjugation length. The estimated β_0 value increases, although not greatly, on moving from **1** to **2**; the effects of the large blue-shift and intensity decrease in the MLCT band are more than compensated for by the accompanying 3-fold increase in $\Delta\mu_{12}$. Comparison of the NLO responses for the new chromophores with those for **1**−**3** is hindered by the necessity for Gaussian fitting that introduces additional uncertainties in the results, as well as the fact that the high-energy ILCT bands could not be analyzed for **4**−**6**. The sums of the two β_0 values derived for **4** and **5** are equivalent (ca. 80×10^{-30} esu) and probably within experimental error of the value measured for **3**. In contrast, the analogous Mebpb$^+$ and Mebph$^+$-based $\{Ru^{II}(NH_3)_5\}^{2+}$ chromophores have Stark-derived β_0 responses over twice that of their Mebpe$^+$ counterpart.[5] The total estimated MLCT-based β_0 response for **6** (ca. 10^{-28} esu) is about the same as that determined for **3** without using spectral deconvolution. However, consideration of the data associated with the ILCT bands for the related $\{Ru^{II}(NH_3)_5\}^{2+}$ and *trans*-$\{Ru^{II}Cl(pdma)_2\}^+$ complexes shows that these transitions can contribute as much as about 35% of the total NLO response.[7,19] The estimated MLCT-based β_0 values for **4**−**6** therefore represent only lower limits.

Conclusions

Three new dipolar complex chromophores containing $\{Fe^{II}(CN)_5\}^{3-}$ electron donor centers coordinated to pyridyl ligands with electron-accepting *N*-methylpyridinium substituents have been prepared and fully characterized. Together with three previously reported related species, these complexes display intense and very broad MLCT absorptions that are strongly solvatochromic. In addition, the MLCT bands show unusual blue-shifts as the conjugation is extended within the polyene series, reminiscent of the behavior of analogous Ru^{II}-based chromophores. HRS studies with a 1064 nm laser reveal relatively large static first hyperpolarizabilities β_0 in both water and methanol. Stark spectroscopic measurements afford dipole moment changes that increase dramatically with chromophore length and also indicate that the MLCT transitions are associated with substantial NLO responses. Single crystal X-ray structures of the materials $Na_2[Fe^{II}(CN)_5(Mepyz^+)]\cdot 9H_2O$ and $Na[Mepyz^+][Fe^{II}(CN)_5(Mepyz^+)]\cdot 3H_2O$ both show some degree of alignment of the constituent complex dipoles. This tendency for non-centrosymmetric crystallization not only encourages further structural studies with related chromophores but could also produce materials with potentially useful macroscopic quadratic NLO properties if large single crystals can be grown.

Acknowledgment. We thank the EPSRC for support in the form of PhD studentships (E.C.H. and C.A.S.) and a postdoctoral grant (SPF, EP/D070732), and also the Fund for Scientific Research-Flanders (FWO-V, G.0297.04), the University of Leuven (GOA/2006/3), and the Belgian Government (IUAP P5/3).

Note Added after ASAP Publication. There was an error in a formula within the Crystallographic Studies section in the version that published on January 12, 2009. The corrected version was published ASAP on January 21, 2009.

Supporting Information Available: X-ray crystallographic data in CIF format. This material is available free of charge via the Internet at http://pubs.acs.org.

IC801224U